Available online at www.sciencedirect.com
ScienceDirect
Journal of Sound and Vibration 322 (2009) 870–882
JOURNAL OF SOUND AND VIBRATION
www.elsevier.com/locate/jsvi

A thermal-energy method for calculating thermoelastic damping in micromechanical resonators

Zhili Hao*, Yang Xu, Shiva Krishna Durgam

Department of Mechanical Engineering, Old Dominion University, 238 Kaufman Hall, Norfolk, VA 23529-0247, USA

Received 15 March 2008; received in revised form 21 November 2008; accepted 2 December 2008
Handling Editor: S. Bolton
Available online 14 January 2009

Abstract

In this paper, a thermal-energy method is presented for calculating thermoelastic damping in micromechanical resonators. In this method, thermoelastic damping is interpreted as the generation of thermal energy per cycle of vibration and consequently is expressed in terms of entropy—a thermodynamic parameter measuring the irreversibility in heat conduction. As compared with a commonly used complex-frequency method, this thermal-energy method does not involve complex values and thus can be implemented in ANSYS/Multiphysics, a finite element modeling software, with fast speed. Based on the governing equations of linear thermoelasticity, the mathematical expressions are first derived for thermoelastic damping in micromechanical resonators made from isotropic and anisotropic materials, respectively. Through two sequential numerical simulations: uncoupled elastic modal simulation and transient heat conduction, the numerical values for these expressions are then calculated in ANSYS/Multiphysics for micromechanical resonators taking different structural geometries. This method is verified using the well-known theoretical solution to thermoelastic damping in a beam resonator and experimental data. As a result, the developed thermal-energy method can calculate thermoelastic damping in micromechanical resonators with any complex structural geometry and made from isotropic and/or anisotropic materials.

1. Introduction

With the advent of the Microelectromechanical Systems (MEMS) technology, micromechanical resonators have been extensively studied for various sensing and wireless communications applications, such as accelerometers [1,2], gyroscopes [3–5], oscillators [6–8], and electrical filters [9,10]. For all these applications, it is important to design and fabricate micromechanical resonators with very high quality factors or very little energy loss, because a high quality factor directly translates to high signal-to-noise ratio, high resolution, and low power consumption. Due to its small size, it is feasible to package a micromechanical resonator in a vacuum and thereby eliminate air damping. Consequently, other loss mechanisms, such as thermoelastic damping (TED), support loss, and surface loss, now come to the fore [11–14], and become major bottlenecks

*Corresponding author. Tel.: +1 757 683 6734; fax: +1 757 683 5344.
E-mail address: zlhao@odu.edu (Z. Hao).

0022-460X/$ - see front matter
doi:10.1016/j.jsv.2008.12.005

for micromechanical resonators' performance. Among these loss mechanisms, TED has been identified as the fundamental limit for the attainable quality factor of a micromechanical resonator [12]. To this end, it is of significant importance to analyze TED, not only for improving the performance of micromechanical resonators, but also for establishing their performance limits.

The laws of thermodynamics predict that a variation of strain in a solid is accompanied by a variation of temperature, which causes an irreversible flow of heat [15]. This heat conduction further gives rise to an increase in entropy and consequently to dissipation of vibration energy. This process of energy dissipation is commonly referred to as *TED*. The theory of thermoelasticity has been well established [16]. The coupled equations of linear thermoelasticity in various infinite geometries have been analytically solved [15,17–19]. However, there are few analytical solutions to TED in finite geometries, in that the repeated reflections of thermoelastic waves at the boundary make the mathematical derivation very complicated [15].

In the 1930s, Zener [20,21] derived an approximate expression for TED in rectangular beams with flexural-mode vibrations. His theory showed that TED in a beam exhibits a Lorentzian behavior with a single thermal relaxation time. This relaxation time is related to the width b of the beam and the thermal diffusivity χ of the structural material used. Currently, TED has received great attention, due to its significance in micromechanical resonators as described above. For instance, Lifshitz and Roukes [12] have provided an exact solution to the thermoelastic equations in micro/nanomechanical beam resonators, predicting a modified Lorentzian behavior of TED, while TED in ring gyroscopes [22,23] has also been addressed.

All the aforementioned works are based on the fundamental assumption that thermoelastic coupling is very weak and has negligible influence on the uncoupled elastic vibration modes of a mechanical resonator, so the elastic and thermal problems are essentially decoupled. Following this assumption, TED is calculated using a complex-frequency method in which TED is expressed in terms of a complex resonant frequency [12]. Recently, the numerical implementation [24] of this method has been conducted in the COMSOL software, where several partial differential equations are numerically solved with complex frequency values being involved. However, our experience shows that implementing large numerical models based on the complex-frequency method is extremely computationally intensive for calculating TED. We reason that this might be due to the fact that a numerical model based on the complex-frequency method needs to deal with complex values. Thus, it is very difficult, if not impossible, to apply the complex-frequency method to TED in those micromechanical resonators with complex structural geometries.

To address this problem, we have developed a thermal-energy method that is based on the very essence of TED: the dissipation of vibration energy is permanently converted into thermal energy. Therefore, one may calculate TED by seeking the generation of thermal energy per cycle of vibration. As compared to the complex-frequency method, this thermal-energy method does not involve complex values and thus can be implemented in ANSYS/Multiphysics with fast speed.

This paper is organized as follows. The following section presents the governing equations of linear thermoelasticity in general. Section 3 presents the thermal-energy method for calculating TED and provides its mathematical expressions. The numerical implementation of this method in a finite element modeling software, ANSYS/Multiphysics, is described in Section 4. The significant insights of this work are concluded at the end.

2. Problem formulation

Although the theory of linear thermoelasticity has been well established and some work has been done on investigating TED in mechanical resonators with different structural geometries, the governing equations of linear thermoelasticity are not comprehensively documented. Thus, this section provides a detailed description of the governing equations of linear thermoelasticity for micromechanical resonators made from isotropic and anisotropic materials, respectively. In particular, due to the popularity of single crystal silicon (SCS) as the structural material for micromechanical resonators, the related governing equations associated with SCS are also included in this section.

2.1. Isotropic materials

Consider a micromechanical resonator made from an isotropic material and initially at a uniform temperature T_0. In a Cartesian coordinate system $x_i = (x_1, x_2, x_3)$, the elastic strain can be expressed in terms of the three displacement components $u_i = (u_1, u_2, u_3)$ in tensor form and vector form, respectively [25]:

$$\varepsilon_{i,j} = u_{i,j} \quad \text{for } i=j \text{ and } \varepsilon_{ij} = \tfrac{1}{2}(u_{i,j} + u_{j,i}) \quad \text{for } i \neq j, \tag{1a}$$

$$\{\varepsilon\}^{\mathrm{T}} = \{\varepsilon_{11} \;\; \varepsilon_{22} \;\; \varepsilon_{33} \;\; \varepsilon_{23} \;\; \varepsilon_{13} \;\; \varepsilon_{12}\}, \tag{1b}$$

where subscripts $i, j = 1, 2, 3$; ε_{ij} is the strain tensor at a point in the resonator; and $u_{i,j}$ (or $u_{j,i}$) denotes the first-order derivative of the ith (or jth) displacement component with respect to the spatial variable x_j (or x_i).

Then, the relations between the elastic stress, the elastic strain, and the temperature variation $\theta = T - T_0$ are written in tensor form and vector form, respectively, as below [25,26]:

$$\sigma_{ij} = 2\mu\varepsilon_{ij} + \lambda\sum_{i=1}^{3}\varepsilon_{ii} - \beta\theta \quad \text{for } i=j \text{ and } \sigma_{ij} = \mu\varepsilon_{ij} \quad \text{for } i \neq j, \tag{2a}$$

$$\sigma^{\mathrm{T}} = [\sigma_{11} \;\; \sigma_{22} \;\; \sigma_{33} \;\; \sigma_{23} \;\; \sigma_{13} \;\; \sigma_{12}], \tag{2b}$$

where λ and μ are Lame coefficients and β is a coefficient related to thermal expansion effect of the resonator. In terms of the material properties, these coefficients can be expressed in three-dimensional (3D) cases and two-dimensional (2D) cases, respectively, as below:

$$\lambda_{3D} = \frac{\upsilon E}{(1+\upsilon)(1-2\upsilon)}, \quad \mu_{3D} = \frac{E}{2(1+\upsilon)} \quad \text{and} \quad \beta_{3D} = \frac{\alpha E}{(1-2\upsilon)}, \tag{3a}$$

$$\lambda_{2D} = \frac{\upsilon E}{1-\upsilon^2}, \quad \mu_{2D} = \frac{E}{2(1+\upsilon)} \quad \text{and} \quad \beta_{2D} = \frac{\alpha E}{(1-\upsilon)}, \tag{3b}$$

where E, υ, and α are the Young's modulus, Poisson's ratio, and linear thermal expansion coefficient of the structural material used, respectively.

According to the Newton's second law, the governing equation of motion in the absence of body forces can be written as

$$\sigma_{ij,j} = \rho\ddot{u}_i, \tag{4}$$

where ρ is the density and the superposed double dot on the displacement component u_i denotes its second-order derivative with respect to time t. Therefore, the governing equation for the elastic vibrations in a micromechanical resonator takes the following format:

$$(\lambda + \mu)u_{j,ij} + \mu u_{i,jj} - \beta\theta_{,i} = \rho\ddot{u}_i. \tag{5}$$

Now, we analyze heat conduction in the micromechanical resonator. According to the Fourier law for heat conduction in isotropic media, the heat flux is related to the temperature gradient by the following expression:

$$q_i = -\kappa\theta_{,i}, \tag{6}$$

where q_i is the ith component of the heat flux vector $\{q\}$ due to the temperature gradient $\theta_{,i}$ along the x_i variable direction and κ, the thermal conductivity of the structural material. As compared to the initial temperature T_0, the temperature variation θ is extremely small. Therefore, based on the definition of entropy, the following relation exists:

$$q_{i,i} = -T_0\rho\dot{s}, \tag{7}$$

where $\dot{s}$ is the rate of the entropy density (Note: the unit of s is $\mathrm{J\,kg^{-1}\,K^{-1}}$).

In the absence of internal heat sources, the governing equation for thermal energy accounting for the interaction between the temperature variation and the elastic strain is written as [27]

$$\rho\dot{s} = \beta\sum_{i=1}^{3}\dot{\varepsilon}_{ii} + \frac{\rho C_P}{T_0}\dot{\theta}, \tag{8}$$

where C_P is the specific heat of the structural material and $\dot{\theta}$ and $\dot{\varepsilon}_{ii}$ are the rate of the temperature variation and the rate of the normal elastic strains, respectively. Combining Eqs. (6)–(8) leads to the governing equation for heat conduction:

$$\kappa\theta_{,ii} - \rho C_P\dot{\theta} = T_0\beta\sum_{i=1}^{3}\dot{\varepsilon}_{ii}. \tag{9}$$

From the above derivation, the governing equations of linear thermoelasticity for a micromechanical resonator made from an isotropic material are summarized as below:

$$(\lambda + \mu)u_{j,ij} + \mu u_{i,jj} - \beta\theta_{,i} = \rho\ddot{u}_i, \tag{10a}$$

$$\kappa\theta_{,ii} - \rho C_P\dot{\theta} = T_0\beta\sum_{i=1}^{3}\dot{\varepsilon}_{ii}. \tag{10b}$$

Note that Eqs. (10) are the same as the governing equations of linear thermoelasticity in scalar form presented in Ref. [24]. While the last term on the left side of the elastic Eq. (10a) represents the stress caused by the temperature variation in the resonator, the term on the right side of the heat conduction Eq. (10b) represents the temperature variation resulted from the elastic dilatation, which is expressed as the summation of the three normal elastic strains $\sum_{i=1}^{3}\varepsilon_{ii}$. These two terms are the factors coupling the elastic vibrations and the temperature variation together.

2.2. Anisotropic materials

Here, we consider a micromechanical resonator made from an anisotropic material and initially at a uniform temperature T_0. The elastic strain in this resonator can be written the same as Eq. (1). Then, the stress caused by the elastic strain and the temperature variation θ is written as

$$\sigma_{ij} = c_{ijkl}\varepsilon_{kl} - \beta_{ij}\theta, \tag{11a}$$

where $i, j, k, l = 1, 2, 3$; c_{ijkl} is the fourth-order tensor of the elastic stiffness and $\beta_{ij} = c_{ijkl}\alpha_{kl}$ is the thermoelastic coupling tensor, where α_{kl} is the thermal expansion tensor. For clarity, the vector form of Eq. (11a) can be written as below:

$$\boldsymbol{\sigma} = \mathbf{c}\boldsymbol{\varepsilon} - \boldsymbol{\beta}\theta, \tag{11b}$$

where

$$\boldsymbol{\beta}^{\mathrm{T}} = [\boldsymbol{\beta}_{11}\ \ \boldsymbol{\beta}_{22}\ \ \boldsymbol{\beta}_{33}\ \ \boldsymbol{\beta}_{23}\ \ \boldsymbol{\beta}_{13}\ \ \boldsymbol{\beta}_{12}], \tag{12}$$

$$\boldsymbol{\alpha}^{\mathrm{T}} = [\boldsymbol{\alpha}_{11}\ \ \boldsymbol{\alpha}_{22}\ \ \boldsymbol{\alpha}_{33}\ \ \boldsymbol{\alpha}_{23}\ \ \boldsymbol{\alpha}_{13}\ \ \boldsymbol{\alpha}_{12}], \tag{13}$$

$$\mathbf{c} = \begin{bmatrix} \mathbf{c}_{11} & \mathbf{c}_{12} & \mathbf{c}_{13} & \mathbf{c}_{14} & \mathbf{c}_{15} & \mathbf{c}_{16} \\ \mathbf{c}_{12} & \mathbf{c}_{22} & \mathbf{c}_{23} & \mathbf{c}_{24} & \mathbf{c}_{25} & \mathbf{c}_{26} \\ \mathbf{c}_{13} & \mathbf{c}_{23} & \mathbf{c}_{33} & \mathbf{c}_{34} & \mathbf{c}_{35} & \mathbf{c}_{36} \\ \mathbf{c}_{14} & \mathbf{c}_{24} & \mathbf{c}_{34} & \mathbf{c}_{44} & \mathbf{c}_{45} & \mathbf{c}_{46} \\ \mathbf{c}_{15} & \mathbf{c}_{25} & \mathbf{c}_{35} & \mathbf{c}_{45} & \mathbf{c}_{55} & \mathbf{c}_{56} \\ \mathbf{c}_{16} & \mathbf{c}_{26} & \mathbf{c}_{36} & \mathbf{c}_{46} & \mathbf{c}_{56} & \mathbf{c}_{66} \end{bmatrix}. \tag{14}$$

Note that the thermoelastic coupling tensor can be further expressed in terms of the elastic stiffness matrix $\boldsymbol{c}$ and thermal expansion vector $\boldsymbol{\alpha}$:

$$\boldsymbol{\beta} = \mathbf{c}\boldsymbol{\alpha}. \tag{15}$$

According to the Newton's second law, the governing equation of motion in the absence of body forces can be written as

$$\sigma_{ij,j} = \rho \ddot{u}_i. \tag{16}$$

Therefore, the governing equation for the elastic vibrations in a micromechanical resonator takes the following format:

$$\rho \ddot{u}_i = \tfrac{1}{2} c_{ijkl}(u_{k,lj} + u_{l,kj}) - \beta_{ij}\theta_{,j}. \tag{17}$$

As to heat conduction in the micromechanical resonator, a modified Fourier law for heat conduction in anisotropic media is written in tensor form and vector form, respectively, as below:

$$q_i = -k_{ij}\theta_{,j}, \tag{18a}$$

$$q = \kappa\{\partial_1 \;\; \partial_2 \;\; \partial_3\}^{\mathrm{T}}\theta, \tag{18b}$$

where

$$\mathbf{q} = \{q_1 \;\; q_2 \;\; q_3\}^{\mathrm{T}}, \tag{19}$$

$$\boldsymbol{\kappa} = \begin{bmatrix} \boldsymbol{\kappa}_{11} & \boldsymbol{\kappa}_{12} & \boldsymbol{\kappa}_{13} \\ \boldsymbol{\kappa}_{21} & \boldsymbol{\kappa}_{22} & \boldsymbol{\kappa}_{23} \\ \boldsymbol{\kappa}_{31} & \boldsymbol{\kappa}_{32} & \boldsymbol{\kappa}_{33} \end{bmatrix}, \tag{20}$$

where $\boldsymbol{\kappa}$ is the thermal conductivity matrix. Based on the definition of entropy, the following relation exists:

$$q_{i,j} = -T_0 \rho \dot{s}, \tag{21}$$

where $q_{i,j}$ is the first-order derivative of the ith component of the heat flux vector $\boldsymbol{\kappa}$ with respect to the x_j variable. In the absence of internal heat sources, the governing equation for thermal energy accounting for the interaction of the temperature variation and the elastic strain is written in tensor form and vector form, respectively, as below:

$$\rho \dot{s} = \beta_{ij}\dot{\varepsilon}_{ij} + \frac{\rho C_P}{T_0}\dot{\theta}, \tag{22a}$$

$$\rho \dot{s} = \boldsymbol{\beta}\dot{\boldsymbol{\varepsilon}}^{\mathrm{T}} + \frac{\rho C_P}{T_0}\dot{\theta}, \tag{22b}$$

where $\dot{\varepsilon}_{ii}$ is the rate of the elastic strain ε_{ij}, and the two vectors $\boldsymbol{\beta}$ and $\boldsymbol{\varepsilon}$ take the form of Eqs. (1b) and (12), respectively. Combining Eqs. (18), (21), and (22) leads to the governing equation for heat conduction in the resonator in tensor form:

$$k_{ij}\theta_{,ij} - \rho C_P \dot{\theta} = T_0 \beta_{ij}\dot{\varepsilon}_{ij}. \tag{23}$$

In summary, the governing equations of linear thermoelasticity for a micromechanical resonator made from an anisotropic material are as follows:

$$\tfrac{1}{2} c_{ijkl}(u_{k,lj} + u_{l,kj}) - c_{ijkl}\alpha_{kl}\theta_{,j} = \rho \ddot{u}_i, \tag{24a}$$

$$k_{ij}\theta_{,jj} - \rho C_P \dot{\theta} = T_0 \beta_{ij}\dot{\varepsilon}_{ij}. \tag{24b}$$

While the second term on the left side of the elastic Eq. (24a) represents the stress caused by the temperature variation, the term on the right side of the heat conduction Eq. (24b) represents the temperature variation resulted from the elastic strain.

2.3. Single crystal silicon

In the MEMS field, SCS has been intensively used as the structural material for micromechanical resonators. Therefore, this subsection focuses upon tailoring the equations in Section 2.2 to SCS resonators. These types of resonators have only three independent elastic constants and its elastic stiffness matrix can be written as below:

$$\mathbf{c} = \begin{bmatrix} \mathbf{c}_{11} & \mathbf{c}_{12} & \mathbf{c}_{12} & \mathbf{0} & \mathbf{0} & \mathbf{0} \\ \mathbf{c}_{12} & \mathbf{c}_{11} & \mathbf{c}_{12} & \mathbf{0} & \mathbf{0} & \mathbf{0} \\ \mathbf{c}_{12} & \mathbf{c}_{12} & \mathbf{c}_{11} & \mathbf{0} & \mathbf{0} & \mathbf{0} \\ \mathbf{0} & \mathbf{0} & \mathbf{0} & \mathbf{c}_{44} & \mathbf{0} & \mathbf{0} \\ \mathbf{0} & \mathbf{0} & \mathbf{0} & \mathbf{0} & \mathbf{c}_{44} & \mathbf{0} \\ \mathbf{0} & \mathbf{0} & \mathbf{0} & \mathbf{0} & \mathbf{0} & \mathbf{c}_{44} \end{bmatrix}. \tag{25}$$

Furthermore, the thermal properties of SCS do not show any dependence on orientations. Consequently, according to Eq. (15), the following expression for $\boldsymbol{\beta}$ can be obtained:

$$\boldsymbol{\beta} = [\mathbf{c}_{11}\boldsymbol{\alpha} + 2\mathbf{c}_{22}\boldsymbol{\alpha} \;\; \mathbf{c}_{11}\boldsymbol{\alpha} + 2\mathbf{c}_{22}\boldsymbol{\alpha} \;\; \mathbf{c}_{11}\boldsymbol{\alpha} + 2\mathbf{c}_{22}\boldsymbol{\alpha} \;\; \mathbf{0} \;\; \mathbf{0} \;\; \mathbf{0}]^{\mathrm{T}}. \tag{26}$$

Thus, the governing equations of linear thermoelasticity for SCS resonators are written as

$$\tfrac{1}{2}c_{ij}(u_{k,lj} + u_{l,kj}) - c_{ij}\alpha_{kl}\theta_{,j} = \rho\ddot{u}_i, \tag{27a}$$

$$\kappa\sum_{i=3}^{3}\theta_{,ii} - \rho C_P\dot{\theta} = T_0(c_{11} + 2c_{12})\alpha\sum_{i=1}^{3}\dot{\varepsilon}_{ii}. \tag{27b}$$

3. Thermal-energy method

As described in Section 2, the governing equations of linear thermoelasticity are well established. Therefore, calculating TED becomes a well-defined problem—solve the two coupled equations for the dissipation of vibration energy per cycle of vibration. So far, TED has been tackled from the perspective of elastic vibrations—the dissipation of vibration energy. In fact, besides interpreted as the dissipation of vibration energy, TED can also be interpreted as the generation of thermal energy per cycle of vibration, which is the very essence of TED [19]. Therefore, one may calculate TED by seeking this generation of thermal energy—referred to as thermal-energy method in this work. This thermal-energy method is based on the well-accepted assumption described previously that thermoelastic coupling is very weak and has negligible influence on the uncoupled elastic mode of a mechanical resonator, so the elastic and thermal problems are essentially decoupled.

Now, we describe the procedure of deriving the mathematical expression for the generation of thermal energy. It should be emphasized that, as compared to the complex-frequency method [12], this thermal-energy method differs in that:

(1) The resonant frequency, elastic vibrations, and temperature variation all hold real values.
(2) While the elastic vibrations are assumed to be time-harmonic, the temperature variation is not time-harmonic any more.

Following the aforementioned assumption, the uncoupled elastic vibration modes from the elastic equation are further assumed and their corresponding elastic strain is derived. Then, the substitution of the elastic strain into the heat conduction equation leads to the expression for the temperature variation in the resonator. Upon knowing the temperature variation, the generation of thermal energy can be derived using a parameter in the thermal field-entropy.

Considering heat conduction in a micromechanical resonator made from an anisotropic material, we can calculate the rate of the total entropy increase S of the whole resonator by irreversible heat conduction [25]:

$$\dot{S} = -\int_V \frac{q_{i,j}}{T}\,\mathrm{d}v = -\int_V \frac{\mathrm{div}(\mathbf{q})}{T}\,\mathrm{d}v = -\int_V \mathrm{div}\left(\frac{\mathbf{q}}{T}\right)\mathrm{d}v + \int_V \mathbf{q}\nabla\left(\frac{1}{T}\right)\mathrm{d}v, \tag{28}$$

where the integrand is integrated across the whole volume of the resonator and T denotes the absolute temperature at a point in the resonator. Upon being transformed into a surface integral, the first integral on the right side of the equation becomes zero because of the adiabatic condition at the boundary of the resonator. Thus, Eq. (28) can be simplified as

$$\dot{S} = \int_V \mathbf{q}\nabla\left(\frac{1}{T}\right)\mathrm{d}v = \int_V \mathbf{q}\frac{\nabla T}{T^2}\,\mathrm{d}v. \tag{29}$$

Based on the definition of entropy, the rate of the generated thermal energy is written as

$$\dot{Q} = \int_V \mathbf{q}\frac{\nabla T}{T}\,\mathrm{d}v = \int_V \boldsymbol{\kappa}\nabla\theta\frac{\nabla\theta}{T_0}\,\mathrm{d}v, \tag{30}$$

where the relation $\theta \ll T_0$ is used. Now, we integrate Eq. (30) over one time period of vibration t_0 and obtain the mathematical expression for TED in a micromechanical resonator made from an anisotropic material:

$$\Delta Q = \int_0^{t_0}\int_V \boldsymbol{\kappa}\nabla\theta\frac{\nabla\theta}{T_0}\,\mathrm{d}v\,\mathrm{d}t. \tag{31}$$

Consequently, for a micromechanical resonator made from a thermally isotropic material or SCS, the above equation can be simplified as below:

$$\Delta Q = \int_0^{t_0}\int_V \frac{\boldsymbol{\kappa}(\nabla\theta)^2}{T_0}\,\mathrm{d}v\,\mathrm{d}t. \tag{32}$$

Once TED ΔQ is obtained, the quality factor related to TED Q_{TED} for a micromechanical resonator can be calculated as

$$Q_{\mathrm{TED}} = 2\pi\frac{W}{\Delta Q}, \tag{33}$$

where W denotes the stored maximum elastic vibration energy per cycle of vibration.

4. Numerical implementation

In order to calculate the mathematical expressions, Eqs. (31) and (32), for TED, we need to conduct the numerical implementation which consists of the following three steps:

(1) We simulate the uncoupled elastic vibrations, Eq. (10a) or (24a) or (27a), in a micromechanical resonator to obtain the elastic strain $\varepsilon_{i,j}$ and the stored maximum elastic vibration energy, W.
(2) The elastic strain obtained from the uncoupled elastic simulation is converted into the internal heat source, according to the following expressions:

$$T_0\boldsymbol{\beta}\dot{\boldsymbol{\varepsilon}}^{\mathrm{T}} \quad \text{(anisotropic materials)}, \tag{34a}$$

$$T_0\beta\sum_{i=1}^{3}\dot{\varepsilon}_{ii} \quad \text{(isotropic materials)}, \tag{34b}$$

$$T_0(c_{11}+2c_{12})\alpha\sum_{i=1}^{3}\dot{\varepsilon}_{ii} \quad \text{(single crystal silicon)}. \tag{34c}$$

(3) To obtain the temperature variation θ, the transient heat conduction, Eq. (10b) or (24b) or (27b), in the resonator with the internal heat source of Eqs. (34), is simulated. Processing the thermal simulation results according to Eq. (31) or (32) gives rise to the calculation of TED, and further leads to the quantitative prediction of the Q_{TED} from Eq. (33).

The above procedure has been implemented in ANSYS/Multiphysics with Element Solid45 for isotropic materials and Element Solid64 for anisotropic materials. Since processing the simulation results virtually takes no time, the running time is approximately the combination of the time for elastic vibrations and that for transient heat conduction, thereby leading to fast speed. Based on this procedure, the Q_{TED} values for micromechanical resonators with different geometries have been simulated. Table 1 summarizes the material properties of the three typical structural materials used in fabrication of micromechanical resonators. Fig. 1 compares the simulated Q_{TED} using the thermal-energy method (with Element Solid45) and the corresponding Q_{TED} from the theoretical solution to beam resonators [12] with different aspect ratios of beam length to beam width (note that the beam width is fixed at 4 μm). This comparison shows excellent agreement toward the right side of the Debye peak, where maximum TED occurs, and thus demonstrates the validity of this method. Now, we address the difference between the simulated Q_{TED} values and the theoretical Q_{TED} values toward the left side of the Debye peak. Note that the dashed lines in Fig. 1 represent the percentage difference between the simulated frequency and the theoretically calculated frequency based on the Euler–Bernoulli beam theory for clamped–free and clamped–clamped beam resonators. These dashed lines clearly show that as the beam length/width ratio decreases (a chubby beam) [28], the percentage difference between the simulated frequency and the theoretically calculated frequency goes up. This indicates that the Euler–Bernoulli beam theory does not hold toward the left side of the Debye peak. Therefore, the difference between the simulated Q_{TED} values and the theoretical Q_{TED} values toward the left side of the Debye peak is due to the fact that the theoretical solution, which is based on the Euler–Bernoulli beam theory, is not valid toward the left side of Debye peak, while the thermal-energy method does not have such limitations.

We further apply this thermal-energy method to other micromechanical resonators with complex geometries. Figs. 2–5 illustrate the simulated elastic vibration modes and energy loss distribution (the integrand in Eq. (32)) due to TED in a tuning-fork structure, a block resonator, and a disk resonator, respectively. The structural geometrical parameters are taken from the literature [6,32–34]. Fig. 6 illustrates the simulated elastic vibration mode and energy loss distribution due to TED in a tuning-fork structure with three flexural beams, which we have recently designed for improving the Q_{TED} in the tuning-fork structure shown in Fig. 2. Its scanning electron microscope (SEM) picture and measured frequency response from a network analyzer are illustrated in Fig. 7.

Table 2 compares the simulated Q_{TED} and the measured quality factor for those micromechanical resonators illustrated in Figs. 2–7, showing good agreement in the sense that the simulated Q_{TED} values are larger than the corresponding measured Q values, which consist of other loss mechanisms, such as support loss and surface loss. In particular, it is found from this comparison that TED is the dominant loss for the two tuning-fork structures shown in Figs. 2, 3, and 6, while it is not a concern for the disk resonator and the block resonator. It is worth mentioning that this numerical implementation is also applicable to a micromechanical

Table 1
Physical properties of three typical structural materials for micromechanical resonators.

Materials	Single crystal silicon [29]	Polysilicon [24]	Polydiamond [30,31]
Poisson's ratio	–	0.22	0.12
Elastic modulus (GPa)	$c_{11}=166$		
	$c_{12}=65$	157	1120
	$c_{44}=80$		
Density ($\mathrm{kg\,m^{-3}}$)	2330	2330	3440
Thermal conductivity ($\mathrm{W\,m^{-1}\,K^{-1}}$)	90	90	1400
Specific heat ($\mathrm{J\,kg^{-1}\,K^{-1}}$)	700	700	565
Linear thermal expansion coefficient ($\mathrm{K^{-1}}$)	2.6×10^{-6}	2.6×10^{-6}	1.0×10^{-6}

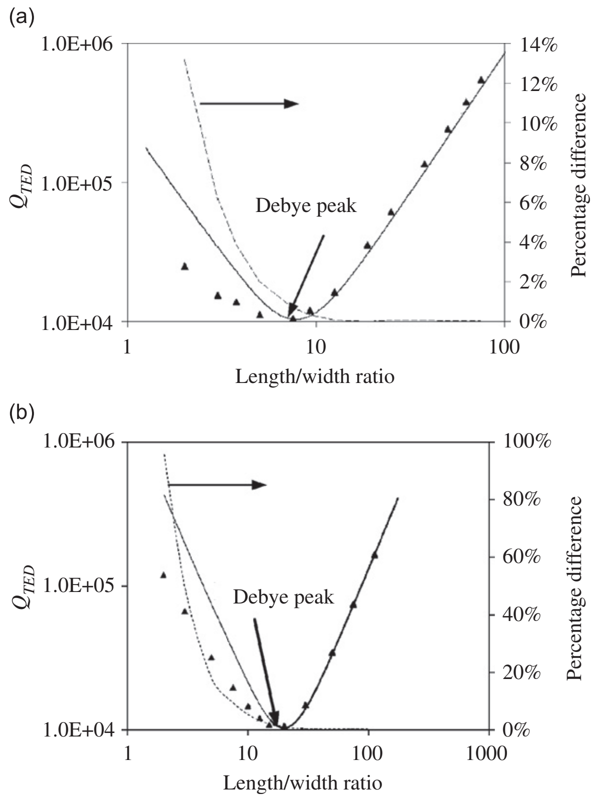

Fig. 1. Comparison between the well-known theoretical solution to the Q_{TED} in a flexural-mode beam resonator and the simulated Q_{TED} using the thermal-energy method (note that polysilicon is assumed to be the structural material and the beam width is fixed at 4 μm): (a) Clamped–free beam and (b) Clamped–clamped beam. — theoretical Q_{TED}; ▲ simulated Q_{TED}; - - - percentage difference between the simulated frequency and the theoretically calculated frequency.

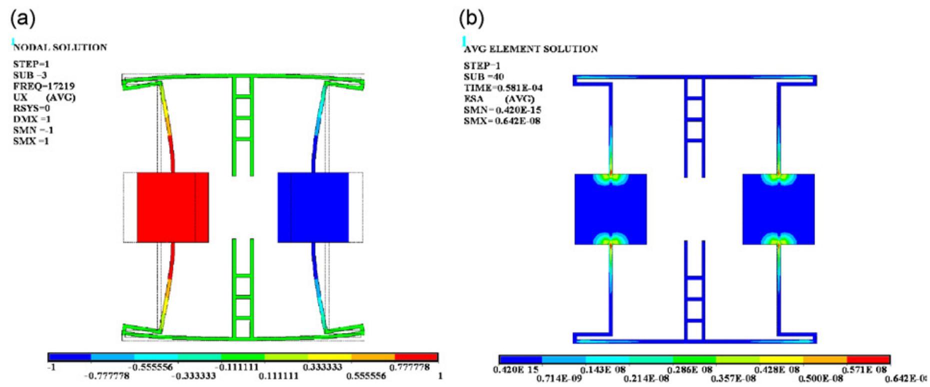

Fig. 2. Simulated elastic vibration mode and energy loss distribution due to thermoelastic damping for the *drive-mode* of a tuning-fork gyroscope made from single crystal silicon: (a) elastic vibration mode and (b) energy loss distribution.

resonator made from different structural materials, as far as the appropriate equations are identified for these materials. Moreover, this thermal-energy method is capable of predicting energy loss distribution due to TED. This feature will facilitate the design optimization of a micromechanical resonator for a higher Q_{TED}.

Since it takes only a few minutes for a personal computer (Intel Core2 Duo 6300 with 2 GB RAM) to calculate TED in those complex geometrical structures with large finite element model sizes (element No.

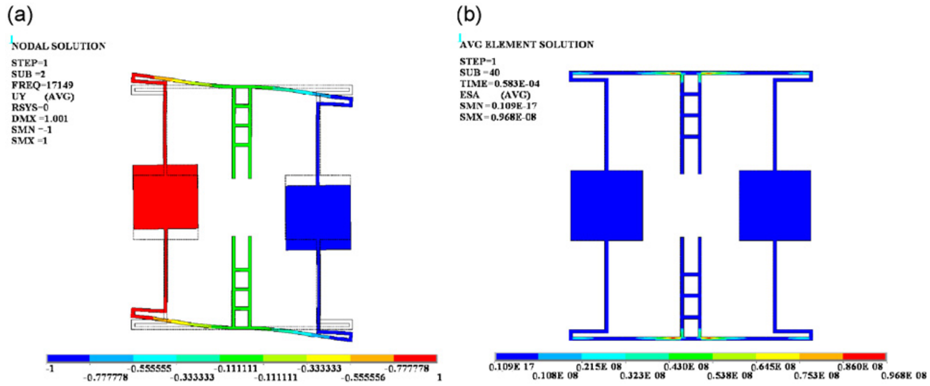

Fig. 3. Simulated elastic vibration mode and energy loss distribution due to thermoelastic damping for the *sense-mode* of a tuning-fork gyroscope made from single crystal silicon: (a) elastic vibration mode and (b) energy loss distribution.

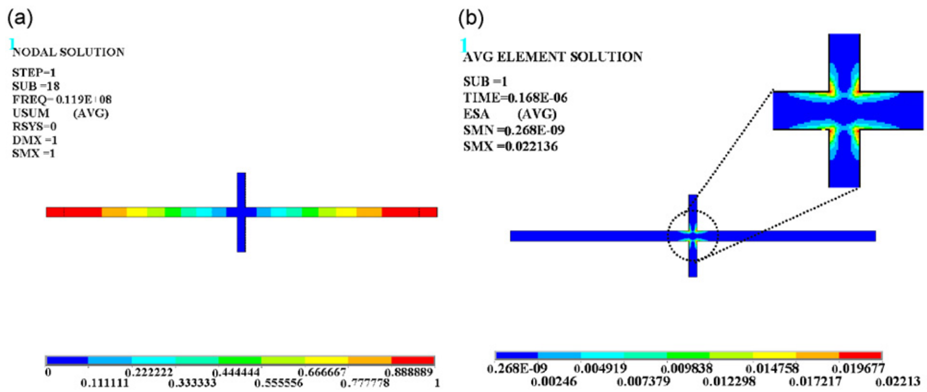

Fig. 4. Simulated elastic vibration mode and energy loss distribution due to thermoelastic damping for a block resonator made from single crystal silicon: (a) elastic vibration mode and (b) energy loss distribution.

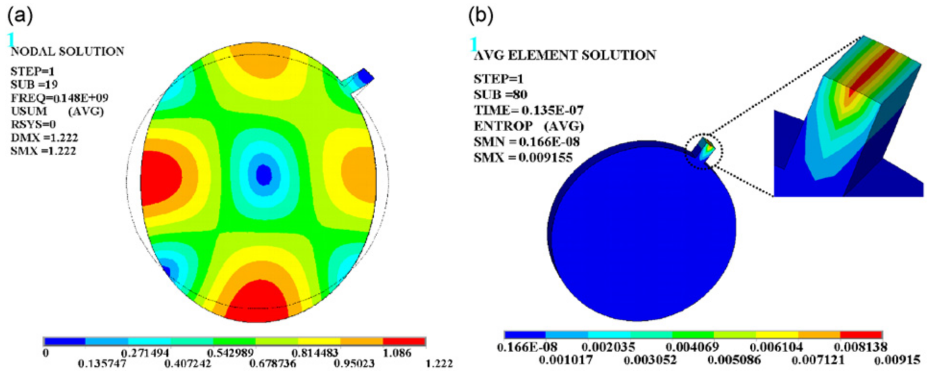

Fig. 5. Simulated elastic vibration mode and energy loss distribution due to thermoelastic damping for a disk resonator with a side-support beam and made from single crystal silicon: (a) elastic vibration mode and (b) energy loss distribution.

>4000) as illustrated in Table 2, this thermal-energy method is very efficient. To further demonstrate great efficiency of this thermal-energy method as compared to the complex-frequency method, we consider a clamped–clamped flexural beam resonator of $400\,\mu m \times 20\,\mu m \times 12\,\mu m$ ($L \times h \times b$) [24]. We simulate TED in this beam resonator with four model sizes in COMSOL using the complex-frequency method and in ANSYS

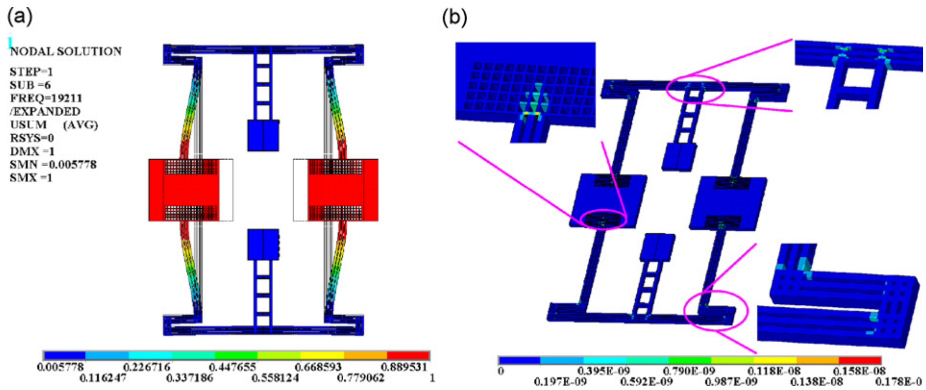

Fig. 6. Simulated elastic vibration mode and energy loss distribution due to thermoelastic damping for a single crystal silicon tuning-fork structure with three flexural beams: (a) elastic vibration mode and (b) energy loss distribution.

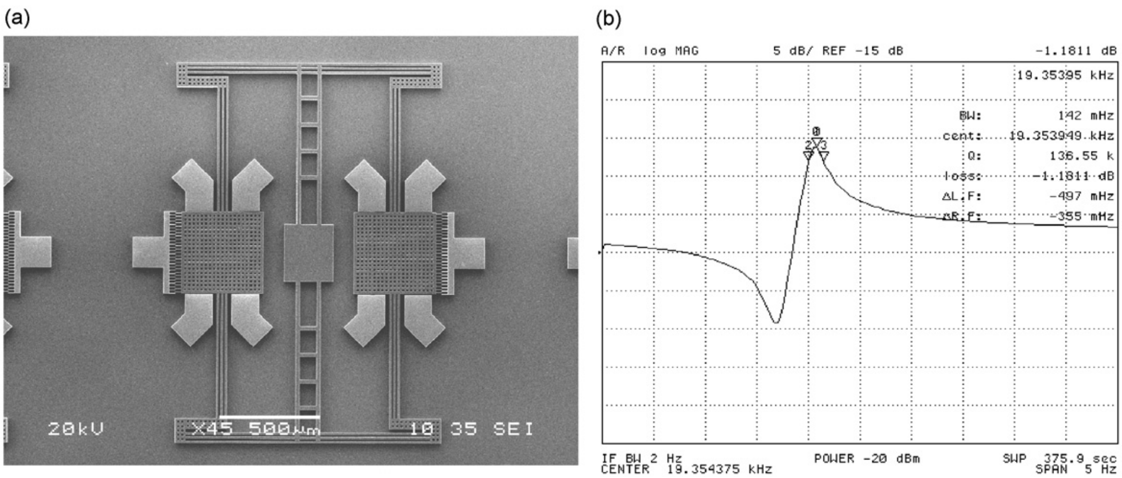

Fig. 7. The scanning electron microscope (SEM) picture and experimental measurement of a tuning-fork structure with three vibration beams: (a) scanning electron microscope picture and (b) the measured frequency response showing $Q_{\mathrm{measured}} = 136{,}550$ at 19.35 kHz.

Table 2
Comparison between the simulated Q_{TED} using the thermal-energy method and the measured Q of micromechanical resonators with different geometries.

Materials	Calculated Q_{TED}	Measured Q	Frequency (kHz)	Element number	Running time (min)
Tuning-fork (drive-mode) [32,33]	87,635	81,000	17,219	4,576	3:09
Tuning-fork (sense-mode) [32,33]	83,563	64,000	17,149	4,576	3:02
Tuning-fork with three flexural beams	176,204	136,550	19,211	4,360	6:23
Block resonator [6]	1,551,876	180,000	11,900	729	0:33
Disk resonator [34]	7,153,088	39,300	148,000	4,440	8:01
Flexural beam resonator [24]	10,439	10,281	636	4,000	2:25

using the thermal-energy method, respectively, with the above-mentioned personal computer. As summarized in Table 3, the running time with different model sizes for these two methods clearly illustrates great efficiency of the thermal-energy method presented in this work.

Table 3
Comparison of the running time between the complex-frequency method implemented in COMSOL and the thermal-energy method implemented in ANSYS for calculating thermoelastic damping in a flexural beam resonator [24] with different model sizes.

	Model size (element no.)			
Running time (s)	200	600	1200	1600
Running time in COMSOL using complex-frequency method	66.89	84.15	105.625	Out of memory
Running time in ANSYS using thermal-energy method	18.26	42.78	51.54	59.22

5. Conclusion

From the perspective of thermal field, a thermal-energy method has been developed for calculating TED in micromechanical resonators. By interpreting TED as the generation of thermal energy per cycle of vibration, this method takes the advantage of a thermodynamic parameter-entropy which quantitatively measures the irreversibility in heat conduction, to formulate TED. Its theoretical derivation and numerical implementation has been described in great details. The validity of this method has been further demonstrated by comparing with the well-known solution to TED in a beam resonator and experimental data. With the advantages of involving no complex values and fast-speed implementation in ANSYS/Multiphysics, this thermal-energy method applies to micromechanical resonators with any complex geometry and made from anisotropic and/or isotropic materials.

Acknowledgment

The authors wish to acknowledge the funding from National Science Foundation (NSF) under Grant no. 0826420.

References

[1] A.A. Seshia, M. Palaniapan, T.A. Roessig, R.T. Howe, R.W. Gooch, T.R. Schimert, S. Montague, A vacuum packaged surface micromachined resonant accelerometer, *Journal of Microelectromechanical Systems* 11 (2002) 784–793.
[2] B.E. Boser, R.T. Howe, Surface micromachined accelerometers, *IEEE Journal of Solid-State Circuits* 31 (1996) 366–375.
[3] N. Yazdi, F. Ayazi, K. Najafi, Micromachined inertial sensors, *Proceeding of IEEE* 86 (1998) 1640–1659.
[4] C. Acar, A.M. Shkel, Inherently robust micromachined gyroscopes with 2-DOF sense-mode oscillator, *Journal of Microelectromechanical Systems* 15 (2006) 380–387.
[5] H. Xie, G.K. Fedder, Fabrication, characterization, and analysis of a DRIE CMOS-MEMS gyroscope, *IEEE Sensors Journal* 3 (2003) 622–631.
[6] T. Mattila, J. Kiihamaki, T. Lamminmaki, O. Jaakkola, P. Rantakari, A. Oja, H. Seppa, H. Kattelus, I. Tittonen, A 12 MHz micromechanical bulk acoustic mode oscillator, *Sensors and Actuators A* 101 (2002) 1–9.
[7] T. Mattila, O. Jaakkola, J. Kiihamaki, J. Karttunen, T. Lamminmaki, P. Rantakari, A. Oja, H. Seppa, H. Kattelus, I. Tittonen, 14 MHz micromechanical oscillator, *Sensors and Actuators A* 97–98 (2002) 497–502.
[8] F.D. Bannon, J.R. Clark, C.T.-C. Nguyen, High-Q HF microelectromechanical filters, *IEEE Journal of Solid-State Circuits* 35 (2000) 512–526.
[9] C.T.-C. Nguyen, Micromechanical resonators for oscillators and filters, *IEEE Ultrasonics Symposium* 1 (1995) 489–499.
[10] K. Wang, C.T.-C. Nguyen, High-order medium frequency micromechanical electronic filters, *Journal of Microelectromechanical Systems* 8 (1999) 534–557.
[11] Z. Hao, A. Erbil, F. Ayazi, An analytical model for support loss in micromachined beam resonators with in-plane flexural vibrations, *Sensors and Actuators A* 109 (2003) 156–164.
[12] R. Lifshitz, M.L. Roukes, Thermoelastic damping in micro- and nanomechanical systems, *Physical Review B* 61 (2000) 5600–5609.
[13] K.Y. Yasutnura, T.D. Stowe, E.M. Chow, T. Pfafman, T.W. Kenny, B.C. Stipe, D. Rugar, Quality factors in micron- and submicron-thick cantilevers, *Journal of Microelectromechanical Systems* 9 (2000) 117–125.
[14] J. Yang, T.T. Ono, M. Esashi, Energy dissipation in submicrometer thick single-crystal silicon cantilevers, *Journal of Microelectromechanical Systems* 11 (2002) 775–783.
[15] I.N. Sneddon, R. Hill, *Progress in Solid Mechanics*, Vol. I, North-Holland, Amsterdam, 1960.
[16] W. Nowacki, *Dynamic Problems of Thermoelasticity*, Noordhoff, Leiden, 1975.
[17] H. Deresiewicz, Plane waves in a thermoelastic solid, *Journal of the Acoustical Society of America* 29 (1957) 204–209.

[18] P. Chadwick, I.N. Sneddon, Plane waves in an elastic solid conducting heat, *Journal of the Mechanics and Physics of Solids* 6 (1958) 223–230.
[19] F.J. Lockett, Effect of thermal properties of a solid on the velocity of Rayleigh waves, *Journal of the Mechanics and Physics of Solids* 7 (1958) 71–75.
[20] C. Zener, Internal friction in solids I. Theory of internal friction in reeds, *Physical Review* 52 (1937) 230–235.
[21] C. Zener, Internal friction in solids II. General theory of thermoelastic internal friction, *Physical Review* 53 (1938) 90–99.
[22] Z. Hao, F. Ayazi, Thermoelastic damping in flexural-mode ring gyroscopes, *Proceedings of ASME 2005 International Mechanical Engineering Congress and Exposition*, IMECE2005-79965, Orlando, FL, November 2005.
[23] S.J. Wong, C.H.J. Fox, S. McWilliam, Thermoelastic damping of the in-plane vibration of thin silicon rings, *Journal of Sound and Vibration* 293 (2006) 266–285.
[24] A. Duwel, R.N. Candler, T.W. Kenney, M. Varghese, Engineering MEMS resonators with low thermoelastic damping, *Journal of Microelectromechanical Systems* 15 (2006) 1437–1445.
[25] L.D. Landau, E.M. Lifshitz, *Theory of Elasticity*, Pergamon Press, London, 1959.
[26] S.D. Panteliou, A.D. Dimarogonas, The damping factor as an indicator of crack severity, *Theoretical and Applied Fracture Mechanics* 34 (2000) 217–223.
[27] H. Al-Qahtani, S.K. Datta, Thermoelastic waves in an anisotropic infinite plate, *Journal of Applied Physics* 96 (2004) 3645–3658.
[28] J.N. Reddy, *An Introduction to the Finite Element Method*, McGraw-Hill, New York, 1984.
[29] L. Börnstein, *Numerical Data and Functional Relationships Science and Technology*, Springer, Berlin, 1979.
[30] J. Philip, P. Hess, T. Feygelson, J.E. Butler, S. Chattopadhyay, K.H. Chen, L.C. Chen, *Journal of Applied Physics* 93 (2003) 2164–2171.
[31] T. Sato, K. Ohashi, T. Sudoh, K. Haruna, H. Maeta, Thermal expansion of a high purity synthetic diamond single crystal at low temperatures, *Physical Review B* 65 (2002) 092102(R).
[32] Z. Hao, M. Zaman, A. Sharma, F. Ayazi, Energy loss mechanisms in a bulk-micromachined tuning fork gyroscope, *Proceedings of the IEEE Sensors Conference*, Daegu, South Korea, October 2006, pp. 1333–1336.
[33] M.F. Zaman, A. Sharma, B.V. Amini, F. Ayazi, Towards inertial grade vibratory microgyros: a high-Q in-plane silicon-on-insulator tuning fork device, *Technical Digest of Solid-State Sensors, Actuators, and Microsystems Workshop*, Hilton Head, SC, June 2004, pp. 384–385.
[34] Z. Hao, F. Ayazi, Support loss in micromechanical disk resonators, *Proceeding of the IEEE Micro Electro Mechanical Systems Conference* (*MEMS'05*), Miami, FL, January 2005, pp. 137–141.